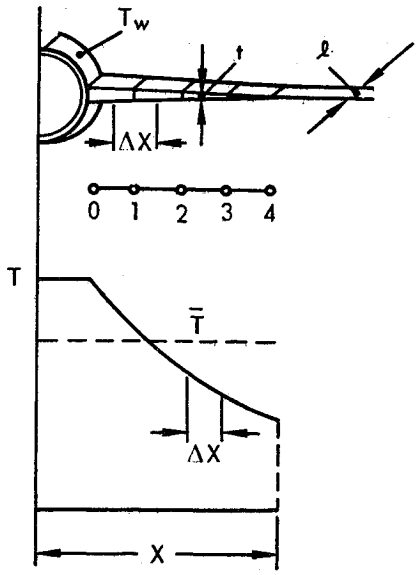

Fig. 1 Radiator element with temperature distribution and average radiating temperature.

Combining Eqs. (1), (5), and (6) yields

$$Q_r = \frac{\pi D^2 V \rho C K}{4}\left[\bar{T}_1 - \left(\frac{\bar{T}_1^3 \pi D^2 V \rho C K}{\pi D^2 V \rho C K + 24\sigma\epsilon B L \bar{T}_1^3}\right)^{1/3}\right] \quad (7)$$

The weight of the radiator and pump is a function of the fluid velocity. This weight is the sum of the weights of the tube, fin, liquid metal, and pump. For a particular radiator, the weights of the fin and liquid metal are fixed. The pump weight is calculated from the pumping power and the specific pump weight in lb/kw of pumping power. The weight of the tube and the pumping power are expressed as a function of fluid velocity by fundamental equations since pressure drop as a function of fluid velocity is expressed by the fundamental equation for incompressible flow. Thus, for a particular radiator and pump, the weight and heat rejected are functions $F(V)$ and $f(V)$, respectively, of the fluid velocity. The specific weight of the radiator is then

$$W_S = W/Q_r = F(V)/f(V) \quad (8)$$

By using the specific pump weight as a parameter, a set of curves with minimum points for the specific weight of the radiator can be constructed from Eq. (8) by varying the fluid velocity.

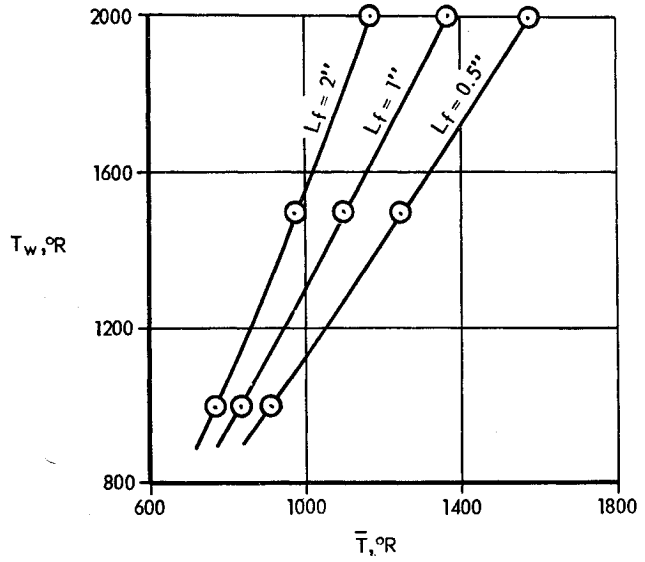

Fig. 2 Average radiating temperature of fin plus tube vs tube wall temperature (emissivity = 0.8).

Conclusions

The technique presented is of value to designers working with liquid-metal, finned beryllium space radiators since it permits a quite rapid optimization calculation of the radiator without the necessity of solving complicated differential equations. The calculated thickness of the tube wall can be increased in order to meet reliability requirements with respect to meteoroid puncture with negligible heat transfer effect since beryllium has good thermal conductivity.

References

[1] Corliss, W. R., *Propulsion Systems for Space Flight* (McGraw-Hill Book Company, Inc., New York, 1960), Chap. 4, p. 126.

[2] Scheiber, L. H., Mitchell, R. P., Gillespie, G. D., and Olcott, T. M., "Techniques for optimization of a finned tube radiator," ASME Paper 61-5A-44 (September 1960).

[3] Wilkins, J. E., Jr., "Minimizing the mass of thin fins," J. Aerospace Sci. **27**, 145–146 (1960).

Hypersonic Wake Characteristics behind Spheres and Cones

ZIGURDS J. LEVENSTEINS*
U. S. Naval Ordnance Laboratory, Silver Spring, Md.

Growth of Turbulent Wake

FROM measurements made from a simultaneously exposed series of shadowgraph photographs of the wake, the width of the turbulent core of the wake δ was determined as a function of x, the downstream distance behind the projectile. Since the edge of the turbulent core is irregular, an averaging process for the determination of the core width was necessary. In this case, the averaging was achieved by tracing the boundary of a 7-in. length of the shadowgraph of the turbulent core with a planimeter. Then the core width δ was obtained by dividing the planimeter reading by the 7-in. length. At the ambient range pressures used (about 40 to 200 mm Hg), no observations were possible with shadowgraph instrumentation for about the first 200 diam behind spheres. However, behind cones the viscous core was clearly visible even at an ambient range pressure of 20 mm Hg.

It has been suggested in Ref. 1 that for incompressible flow the width of the turbulent core δ is proportional to the cube root of (xC_DA), where C_D is the drag coefficient of the body and A the area on which the drag coefficient is based. In an equation form, this can also be written as

$$(\delta/d)/C_D^{1/3} = K(x/d)^{1/3} \quad (1)$$

where d is the body diameter and K a constant of proportionality. Figure 1 shows a log-log plot of $(\delta/d)C_D^{-1/3}$ vs x/d of the Naval Ordnance Laboratory results for both spheres and cones. Also shown in the figure are the freestream Mach numbers M_∞ and freestream Reynolds numbers based on body diameter $R_{\infty d}$, at which the data were obtained. For the spheres, a constant drag coefficient of 0.9 was used. The drag coefficients for the 8° half-angle cones, including induced pressure and transverse curvature effects, were theoretically computed.[2] As can be seen from Fig. 1, when nondimensionalized in this fashion, the widths of the turbulent core of the wake behind both blunt and slender bodies collapse on a single curve. The equation of the curve which best describes the experimental results is

$$(\delta/d)/C_D^{1/3} = 0.9(x/d)^{1/3} \quad (2)$$

Received August 21, 1963. The author expresses his gratitude to R. E. Wilson for his helpful suggestions and discussions of the subject.

* Aerospace Research Engineer. Member AIAA.

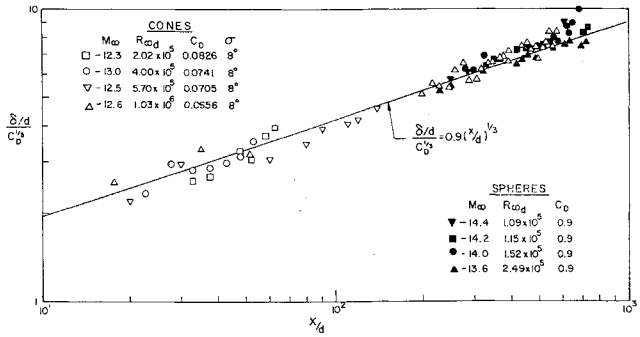

Fig. 1 Sphere and cone wake turbulent core growth results obtained in the Naval Ordnance Laboratory ballistic ranges.

For the near-wake region, when x/d is less than about 1000, such behavior of the hypersonic wake has not been expected from theoretical considerations.[3]

Figure 2 shows a similar correlation of turbulent core width data obtained by Slattery and Clay,[4] although when x/d is less than 100, there is a great deal of scatter of the results. The data were obtained over a wide freestream Reynolds number range and at freestream Mach number 5 for the cones and 7.7 for the spheres. The drag coefficients for the 12.5° half-angle cones were theoretically computed by including pressure, skin friction, and base drag effects. The constant of proportionality K in Eq. (1) which fits these results is 0.7. For comparison, two other curves are included in Fig. 2: a curve with $K = 0.9$ describing Naval Ordnance Laboratory results obtained at Mach numbers from $M_\infty = 12.3$ to 14.4, and the curve describing the turbulent core growth behavior of an incompressible wake. The latter one is Townsend's solution for the axisymmetric wake,[1] where the value of K equal to 0.47 was computed by setting the equilibrium flow constant R_T', which appears in Townsend's solution, equal to the experimentally measured value of 14.1 and setting the virtual origin of the wake x_0 equal to zero. A few core width data points obtained at Naval Ordnance Laboratory ballistics ranges from low supersonic Mach number sphere firings also fall on Townsend's curve. Thus, it appears that the growth behavior of the turbulent core in the near-wake region ($x/d < 1000$) for both sphere and slender cone wakes can be described by an equation of the form

$$(\delta/d)/C_D^{1/3} = f(M_\infty)(x/d)^{1/3} \qquad (3)$$

where $f(M_\infty)$ is some Mach number dependent function.

Laminar to Turbulent Transition in the Cone Wake

The length of laminar flow in the viscous core of the wake behind cones was measured on shadowgraph photographs obtained from hypervelocity firings of 6.3° and 8° half-angle cones in the Naval Ordnance Laboratory ballistics ranges. Figure 3 is a typical shadowgraph of an 8° half-angle cone

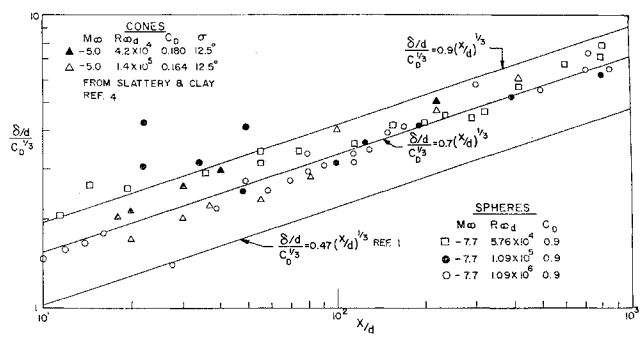

Fig. 2 Sphere and cone wake turbulent core growth results obtained in Lincoln Laboratory ballistics ranges and comparison of these results with Naval Ordnance Laboratory hypersonic and Townsend's incompressible results.

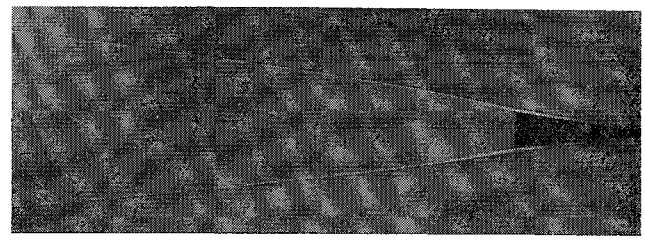

Fig. 3 Shadowgraph of wake behind an 8° half-angle cone flying in the Naval Ordnance Laboratory ballistics range at $M_\infty = 13$ and $p_\infty = 150$ mm Hg.

wake at $M_\infty = 13$ and ambient range pressure $p_\infty = 100$ mm Hg. There were two length measurements made: x_1, the distance from the cone to the first appearance of instability in the laminar flow of the viscous core, and x_2, the distance from the cone to where the flow in the viscous core appears to have become fully turbulent.

Both the x_1, the incipient transition data, and x_2, the fully turbulent transition data, were correlated by forming the wake transition Reynolds numbers $R_{\infty x_1}$ and $R_{\infty x_2}$, respectively, and plotting them vs the freestream body Reynolds number $R_{\infty d}$. Figure 4 shows the incipient transition Reynolds number results. The solid symbol in the $\sigma = 6.3°$ half-angle cone results represents a cone with a base diameter of 0.444 in. The open symbols are for 0.222-in. base diameter cones. The base diameters for the 8° half-angle cones were 0.400 in., and the variation in the body Reynolds number was obtained by ambient range pressure variation. For the two 8° half-angle cone points with upward facing arrows, no transition distance could be measured because it was longer than the length of the 17-in. photographic plates. Hence, the incipient transition Reynolds numbers for these two points are at least as large as indicated in Fig. 4. Also included in the figure are some incipient transition results for 10° half-angle cones obtained at various freestream Mach and Reynolds numbers in the Avco Research and Advanced Development ballistics ranges.[5] Figure 5 is a similar correlation for $R_{\infty x_2}$, the fully turbulent transition Reynolds number results. In addition to the NOL and Avco/RAD results, there are also shown transition results obtained by Slattery and Clay in the Massachusetts Institute of Technology Lincoln Laboratory's ballistics ranges.[4] The open symbols represent $\frac{3}{8}$-in. and the solid symbols $\frac{3}{16}$-in. base diameter 12.5° half-angle cones. Both Avco/RAD and Lincoln Laboratory transition data were obtained from measurements made on schlieren photographs of the wake.

From both the incipient transition and fully turbulent transition data correlations, Figs. 4 and 5, it appears that there exists a constant freestream wake transition Reynolds number independent of freestream body Reynolds number but strongly influenced by the freestream Mach number.

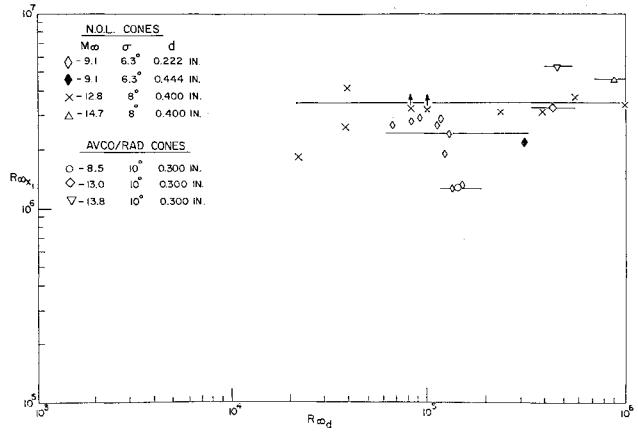

Fig. 4 Correlation of incipient wake transition Reynolds number.

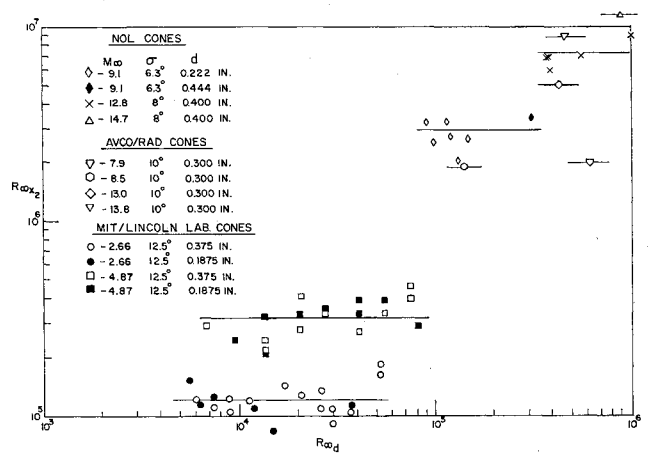

Fig. 5 Correlation of fully turbulent wake transition Reynolds number.

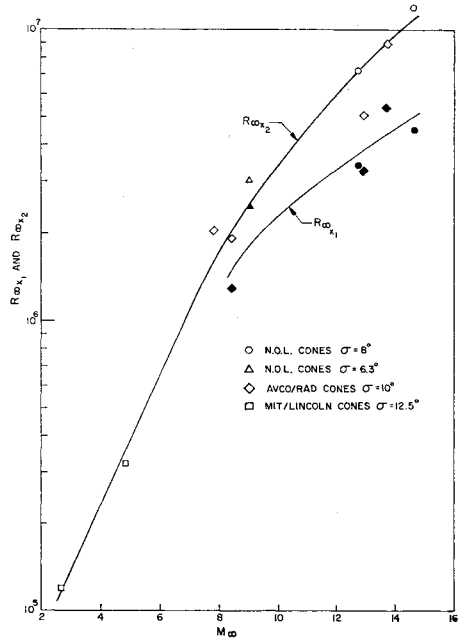

Fig. 6 Effect of freestream Mach number on wake transition Reynolds numbers.

The existence of a constant transition Reynolds number, independent of body diameter, was mentioned by Lees[6] in his description of a hypersonic wake flow model. From a correlation of blunt body wake transition data, Demetriades and Gold found a similar result.[7, 8]

The values of both wake transition Reynolds numbers $R_{\omega x_1}$ and $R_{\omega x_2}$ as functions of the freestream Mach number are shown in Fig. 6. The solid symbols represent the incipient transition Reynolds numbers, and the open symbols represent the fully turbulent ones. It appears that the transition zone of the viscous core increases in length with an increase of the freestream Mach number.

References

[1] Townsend, A. A., *The Structure of Turbulent Shear Flow* (Cambridge University Press, Cambridge, England, 1956), Chap. VII, pp. 169–171.

[2] Lyons, W. C., private communication, Naval Ordnance Lab. (1963).

[3] Hromas, L. and Lees, L., "Effect of nose bluntness on the turbulent hypersonic wake," Space Technology Labs. Rept. 6130-6259-KU-000 (October 1962).

[4] Slattery, R. E. and Clay, W. G., "The turbulent wake of hypersonic bodies," ARS Preprint 2673-62 (1962).

[5] Pallone, A. J., Erdos, I. I., Eckerman, J., and McKay, W., "Hypersonic laminar wakes and transition studies," AIAA Preprint 63-171 (1963).

[6] Lees, L., "Hypersonic wakes and trails," ARS Preprint 2662-62 (1962).

[7] Demetriades, A. and Gold, H., "Transition to turbulence in the hypersonic wake of blunt-bluff bodies," ARS J. **32**, 1420–1421 (1962).

[8] Demetriades, A. and Gold, H., "Correlation of blunt-bluff body wake transition data," Graduate Aeronaut. Lab., Calif. Inst. Tech. Internal Memo. 12 (September 1962).

Shock Curvature Effect on the Outer Edge Conditions of a Laminar Boundary Layer

IRVING RUBIN*
Republic Aviation Corporation, Farmingdale, N. Y.

Nomenclature

C_D = drag coefficient of spherical segment
$f(\eta)$ = dimensionless stream function
R = nose radius of the body
r = radial coordinate of the body
Re_R = Reynolds number based on nose radius
s = coordinate along the body surface
u = velocity
x = coordinate along the body axis of symmetry
y = radial coordinate of the shock wave
δ = boundary-layer thickness
θ_c = cone half-angle
θ_{sh} = local shock-wave angle
μ = absolute viscosity
ρ = density
ψ = stream function

Subscripts

∞ = freestream condition
e = condition at outer edge of boundary layer

PREDICTION techniques for aerodynamic heating are dependent on the boundary-layer outer edge conditions. The method by which these conditions are obtained will therefore influence the magnitude of the computed heat-transfer rates. Thus, consider the region of simple blunted shapes several nose diameters or more downstream of the stagnation point. The boundary-layer outer edge conditions may be obtained here by either assuming an attached shock wave or by expanding isentropically from the normal shock conditions at the nose stagnation point to the known local pressure. The resulting heat-transfer rates will be quite different depending on the method used.

Since the first method applies far downstream of the stagnation region and the second method applies in the vicinity of the nose or leading edge, there exists a substantial region along the body where the outer edge conditions, and hence the heating rates, are intermediate to the forementioned two extremes.

A method for determining the variation of the flow conditions at the outer edge of a laminar boundary layer over a blunted cone resulting from entropy gradients due to shock wave curvature is presented in Ref. 1. The method is derived for a perfect gas, and the reported results were obtained using an electronic computer.

The purpose of this note is to point out a simple approach for solving this problem graphically, which includes real gas effects, and to indicate the effect resulting from the perfect gas assumption in the hypersonic flow regime.

Received August 23, 1963.

* Principal Thermodynamics Engineer, Paul Moore Research and Development Center. Member AIAA.